DOI: 10.1002/ejic.200800700

A Combined Gas-Phase Electron Diffraction/Mass Spectrometric Study of the Sublimation Processes of $TeBr_4$ and TeI_4: The Molecular Structure of Tellurium Dibromide and Tellurium Diiodide

Sergey A. Shlykov,*[a] Heinz Oberhammer,[b] Anton V. Titov,[a] Nina I. Giricheva,[c] and Georgiy V. Girichev[a]

Keywords: Tellurium halides / Gas-phase electron diffraction / Mass spectrometry / Quantum chemical calculations

The sublimation processes of $TeBr_4$ at 471(5) K and TeI_4 at 373(5) K were studied with a combined gas-phase electron diffraction and mass spectrometric technique (GED/MS). The mass spectra and the analysis of the GED intensities showed that a contribution of 40(3) mol-% $TeBr_2$, 59(3) mol-% Br_2, and 1 mol-% $TeBr_4$ was formed in the vapor over $TeBr_4$(s). Solid tellurium tetraiodide decomposes to form I_2(g) and Te(s). A very small contribution of 3.3 ± 2.1 mol-% of gaseous TeI_2 was also determined by both GED and MS. The "metallic" Te accumulated in the solid phase vaporizes at above ca. 670 K as the predominately Te_2 molcular species. Refinement of the GED intensities resulted in r_g(Te–Br) = 2.480(5) Å and $\angle_g$Br–Te–Br = 99.0(6)° for $TeBr_2$ and r_g(Te–I) = 2.693(9) Å and $\angle_g$(I–Te–I) = 103.1(22)° for TeI_2. The small contribution of $TeBr_4$ observed in the mass spectra of the vapor over $TeBr_4$ could not be observed in the GED data. Geometric parameters and vibrational frequencies for the tellurium dihalides TeX_2 with X = F, Cl, Br, and I were calculated with B3LYP, MP2, CCSD, and CCSD(T) methods by using aug-cc-pVTZ basis sets and various core potentials for the tellurium atom. Bonding properties in tellurium dihalides are discussed on the basis of natural bond orbital analyses.

Introduction

Solid selenium and tellurium tetrafluoride and tetrachloride are known to sublime in vacuo at moderate temperatures as monomeric EX_4 gaseous species. In contrast, the bromides and iodides of both chalcogens are less stable and, therefore, decompose, at least, partially when transferred to the gas phase.

The first gas-phase electron diffraction (GED) investigation of tellurium dihalides was performed in 1936 by Grether,[1] who reported values of r(Te–C1) = 2.36 ± 0.03 Å, r(Te–Br) = 2.49 ± 0.03 Å, ∠Br–Te–Br and ∠CI–Te–C 1 > 150°. A decade later Rogers and Spurr[2] re-determined the structure of $TeBr_2$ also by GED, and the r(Te–Br) distance was found to be 2.51 ± 0.02 Å, but the angle Br–Te–Br of 98 ± 3° was much smaller than that predicted for the almost linear structure reported by Grether.[1] In both studies, samples of TeX_2 were used. Much later, Fernholt et al.[3] performed a high level GED study of the vapor of a liquid sample with the composition Te/Cl = 1:2 at 483 K and found it to consist of $TeCl_2$ molecules with a bond length r_a(Te–Cl) = 2.329 ± 0.003 Å and a valence angle $\angle_a$Cl–Te–Cl = 97.0 ± 0.6°.

Basciani and Ferro[4] investigated the sublimation of tellurium tetrabromide at 423–485 K by the torsion-effusion method and found that $TeBr_4$(s) decomposes predominantly to gaseous $TeBr_2$(g) and Br_2(g), with a minor contribution of gaseous tetrabromide. D′Alessio et al.[5] studied the sublimation of $TeCl_4$ and TeI_4 by the torsion-effusion method and established that $TeCl_4$ sublimes congruently, whereas TeI_4(s) decomposes in the temperature range 340–396 K predominantly to Te(s) and I_2(g), with a minor amount of TeI_2(g). Two vibrational frequencies, ν_1 = 377 and ν_2 = 125 cm^{-1}, were reported by Beattie and Perry,[6] which were observed in the gas-phase Raman spectra of $TeCl_2$.

Since solid $TeBr_4$ and TeI_4 are known to undergo considerable decomposition upon evaporation it is necessary to apply a special technique for accurately monitoring the composition of the particular vapors under investigation. In both early GED investigations of $TeBr_2$, the values for the Te–Br distance were reported with large (≈1%) uncertainties[1,2] and with the bond angles contradicting each other. Only two vibrational frequencies are known from the

[a] Department of Physics, Ivanovo State University of Chemistry and Technology,
Engels av. 7, Ivanovo 153000 Russia
Fax: +7-4932-41-79-95
E-mail: shlykov@isuct.ru
[b] Institut für Physikalische und Theoretische Chemie, Universität Tübingen,
72076 Tübingen, Germany
Fax: +49-7071-295490
E-mail: heinz.oberhammer@uni-tuebingen.de
[c] Department of Physical Chemistry, Ivanovo State University,
Ermaka st. 39, Ivanovo 153025 Russia
E-mail: g.v.grichev@mail.ru

Raman spectra of $TeCl_2$ and none for other tellurium dihalides. Furthermore, to the best of our knowledge, no mass spectrometric study was published for any of the tellurium dihalides. In the present investigation, we employed a unique apparatus which combines gas-phase electron diffraction and mass spectrometry (GED/MS) to study the molecular structure of $TeBr_2$. Furthermore, we made an attempt to find conditions at which the structure of TeI_2 could be determined. In addition, we performed a series of high-level quantum chemical (QC) calculations for TeX_2 molecules, where X = F, Cl, Br, I, in order to explore the tendencies and correlations in the geometry, vibration, and electronic structure within this series.

Results and Discussion

Structural Analysis

Vapor Over $TeBr_4$(s)

According to the mass spectra (Table 1) recorded simultaneously with the diffraction experiment, $TeBr_4$ undergoes a decomposition when heated in vacuo, and the vapor over solid tellurium tetrabromide consists predominantly of the dissociation products, $TeBr_2$ and Br_2. A least-squares analysis of the experimental $sM(s)$ function was performed with a modified version of the KCED program.[18] A complex vapor composition was taken into account by applying the expression in Equation (1), where α is the coefficient that gives the contribution of an individual $sM(s)$ functions to the total one.

$$sM_{theor}(s) = \alpha sM_{theor}(s)_{TeBr_2} + (1-\alpha)sM_{theor}(s)_{Br_2} \quad (1)$$

Since this molecular intensity function is derived from the total intensity in the way shown in Equation (1), the real concentrations of the molecular species differ from the α coefficients because of different atomic scattering functions for the species with different atomic composition. The procedure for transforming these coefficients to mol fractions was described earlier by Girichev.[19] The following parameters were refined independently: the α coefficient, bond lengths r(Te–Br) and r(Br···Br), and vibrational amplitudes l(Te–Br) and l(Br···Br) of $TeBr_2$. The results of the least-squares refinement of the $sM(s)$ functions for long (L_1 = 598 mm) and short (L_2 = 338 mm) camera distances, along with the results of joint refinement of both data sets are given in Table 2. Structural parameters in terms of an effective g structure of $TeBr_2$ are presented in Table 3. Radial distribution functions are plotted in Figure 1.

Table 2. Results[a] of the least-squares refinement of the experimental $sM(s)$ functions for the mixture of $TeBr_2$ and Br_2.

	"$TeBr_2$ + Br_2"[b]	"$TeBr_2$ + Br_2"[c]	"$TeBr_2$"[d]
r_a(Te–Br)	2.4789(2)	2.4790(2)	2.4570(14)
r_a(Br···Br)	3.7641(20)	3.7641(20)	3.7660(148)
l(Te–Br)	0.0614(3)	0.0618(3)	0.0911(18)
l(Br···Br)	0.1611(16)	0.1614(16)	0.1794(117)
$r_a(Br–Br)_{Br_2}$	[2.2895]	2.2875(6)	–
$l(Br–Br)_{Br_2}$	[0.0531]	0.0535(6)	–
$\alpha(TeBr_2)$	0.564(2)	0.565(2)	[1.00]
mol-%($TeBr_2$)[e]	38.2(6)	38.3(6)	[100]
R_f [%]	2.9	2.9	19.5

[a] Joint refinement of both short and long camera distances are represented; internuclear distances and amplitudes in Å; standard deviations σ_{LS} of the least-squares procedure are given in parentheses for the refined parameters (distances, amplitudes, and α), except the mol% value for which the $3\sigma_{LS}$ is given; the minor amount of $TeBr_4$ was included into the refinement scheme in a separate analysis (see Results and Discussion). [b] Refinement of all parameters; those for molecular bromine were fixed. [c] Refinement of all parameters including those for molecular bromine; the amplitudes l(Te–Br) in $TeBr_2$ and l(Br–Br) in Br_2 were refined in a group. [d] Refinement performed under assumption that the vapor contains the species $TeBr_2$ only. [e] Conversion of the contribution α of the molecular species to the $sM(s)$ function [see Equation (1)] into the mol fraction value was performed according to the procedure described in Ref.[19]

The molecular parameters of Br_2 are known from spectroscopic data and are readily available.[20] On the basis of these data, the effective molecular parameters of bromine, r_a(Br–Br) = 2.2895 Å and l(Br–Br) = 0.0531 Å, and the asymmetry constant (2.7×10^{-6} Å^3) have been calculated for the temperature at which the GED/MS experiment was performed (471 K). The parameters for $TeBr_2$ obtained in different least-squares analyses, in which the molecular parameters for Br_2 were set to the above values (column 1 in

Table 1. Electron impact (U_i = 50 V) mass spectra of the vapors effused from the cell filled with solid $TeBr_4$ recorded during the combined GED/MS experiment.[a]

Ion	L_1	L_2
Br^+	29.7 ± 8.5	36.3 ± 1.3
Te^+	36.0 ± 3.5	38.8 ± 1.7
Br_2^+	97.3 ± 4.0	98.6 ± 1.6
$TeBr^+$	100	100
$TeBr_2^+$	46.9 ± 0.9	47.5 ± 0.8
$TeBr_3^+$	4.5 ± 0.6	4.3 ± 0.1
Concentration [mol-%][b]	42.3 ± 2.3;56.4 ± 2.3; 1.3 ± 0.2	41.1 ± 0.9; 57.7 ± 0.9; 1.2 ± 0.1

[a] Relative peak intensities. The natural isotopic distributions were taken into account. The values of uncertainties are the statistical errors of several mass spectroscopic runs obtained simultaneously with the diffraction patterns. [b] The concentrations calculated on the basis of the atomic ionization cross-sections additive scheme are given in the sequence $TeBr_2$, Br_2, and $TeBr_4$.

Table 3. Experimental and calculated geometric and vibrational parameters[a] for tellurium dihalides.

Method	ECP on Te[d]	r(Te–X)	∠X–Te–X	l(Te–X)[e]	l(X···X)[e]	$\nu_1(A_1)$	$\nu_2(A_1)$	$\nu_3(B_2)$
				TeF_2				
B3LYP	ECP–46	1.892	94.8			643	210	623
MP2	ECP–46	1.887	94.6			655	214	639
CCSD	ECP–46	1.877	93.7			672	221	655
CCSD(T)	ECP–46	1.886	94.0			654	214	639
				$TeCl_2$				
B3LYP	ECP–46	2.339	99.7	0.058	0.158	377	126	359
	ECP–28	2.357	100.1	0.059	0.170	370	118	348
MP2	ECP–46	2.318	98.2	0.054	0.151	402	132	387
CCSD	ECP–28	2.330	97.9	0.055	0.152	393	132	380
CCSD(T)	ECP–46	2.331	98.3	0.056	0.154	389	129	376
Experiment								
GED (r_g, $\angle_g$)[b]		2.331(3)	97.2(6)	0.070(2)	0.152(14)			
Raman[c]						377	125	
				$TeBr_2$				
B3LYP	ECP–46	2.496	101.1	0.061	0.168	256	82	250
MP2	ECP–46	2.470	99.1	0.057	0.162	273	85	269
	ECP–28	2.474	98.9	0.057	0.162	272	85	268
CCSD	ECP–46	2.482	99.3	0.058	0.162	267	85	265
	ECP–28	2.487	99.0	0.058	0.162	267	85	265
CCSD(T)	ECP–46	2.488	99.4	0.059	0.167	262	83	260
	ECP–28	2.495	99.2	0.060	0.169	260	82	257
Experiment								
GED (r_g, $\angle_g$)[f]		2.480(5)	99.0(6)	0.061(1)	0.161(5)			
				TeI_2				
B3LYP	ECP–46	2.712	102.9	0.060	0.164	198	61	198
MP2	ECP–46	2.685	100.2	0.057	0.160	212	63	213
CCSD(T)	ECP–46	2.709	100.6	0.059	0.166	201	61	203
Experiment								
GED (r_g, $\angle_g$)[f]		2.693(9)	103.1(22)	0.059(6)	0.190(65)			

[a] Distances and amplitudes in Å, angles in degrees, frequencies in cm^{-1}. [b] The r_a and $\angle_a$ values given in Ref.[3] (GED, T = 483 K) were recalculated in this work to give the r_g and $\angle_g$ values given here. [c] Raman spectroscopy, gas, Ref.[6] [d] See the section "Quantum Chemical Calculations" for details and abbreviations. [e] The theoretical amplitudes calculated using the SHRINK program of Sipachev[21] for the temperatures of the GED experiments (483 K $TeCl_2$,[3] 471 K $TeBr_2$, and 373 K TeI_2) from a harmonic force field obtained in the quantum chemical calculations. [f] The experimental GED data obtained in this work are supplied with the uncertainties that were taken as: $\Delta r = [\sigma_{scale}^2+(2.5\sigma_{LS})^2]^{1/2}$, where $\sigma_{scale} = 0.002r$ and σ_{LS} is a standard deviation in least-squares refinement; $\Delta l = 3\sigma_{LS}$; $\Delta\angle$ was calculated from the uncertainties in the internuclear distances.

Table 2) or refined (column 2 in Table 2), are the same within their combined standard deviations. This demonstrates that scale uncertainties of the apparatus or refinement procedures are negligible. Practically no high correlation between parameters occurred in the least-squares refinement. The strongest correlation coefficients were –0.41 for a/r(Te–Br) and 0.64 for a/l(Te–Br).

Since our MS data indicate the presence of a small amount of $TeBr_4$ in the vapor over solid tellurium tetrabromide, in addition to $TeBr_2$ and Br_2, it seemed reasonable to test the sensitivity of the least-squares refinement to this minor species. In order to introduce $TeBr_4$ into the least-squares refinement, the MP2 data were used after calculating vibrational amplitudes and corrections by means of the Sipachev's program SHRINK.[21] Since the MP2 approximation reproduces the experimental parameters for $TeBr_2$ better than the B3LYP method (see Table 3), it also appears to be more suitable for $TeBr_4$. Results of these least-squares analyses are described below.

Vapor Over TeI_4(s)

Refinement of the data showed that the experimental molecular intensities are perfectly described with the assumption that the vapor over solid TeI_4 consists only of I_2 molecules with an agreement factor R_f = 2.9%. The effective parameters r_g(I–I) = 2.672(5) Å and l(I–I) = 0.060(1) Å and the asymmetry constant $B = 5(9)\times10^{-7}$ Å^3 are in excellent agreement with those obtained at 353 K by Ukaji and Kuchitsu:[22] r_g(I–I) = 2.672(3), l(I–I) = 0.061(5) Å, and $B = 39(84)\times10^{-7}$ Å^3.

An attempt to determine the structural parameters of TeI_2 was complicated because of the fact that the bond length r(I–I) in molecular iodine is very close to the bond length r(Te–I) in TeI_2. As can be seen from the results of the QC calculations (Table 3), these values differ by less than 0.03 Å. The (I···I) distance in tellurium diiodide, which occurs far from the bonded distances in the radial distribution function, might, therefore, be refined independently.

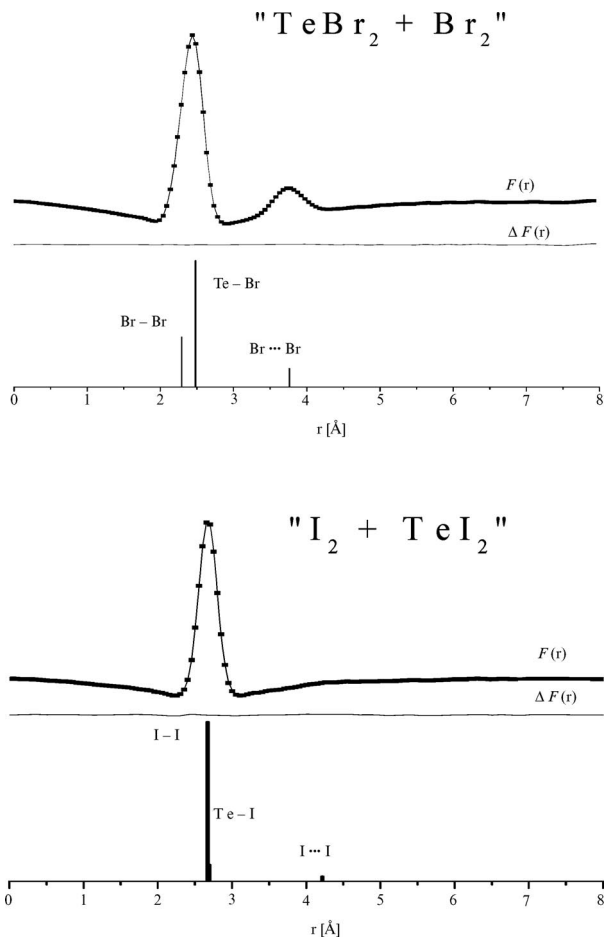

Figure 1. Radial distribution curves $F(000)r$ of the gaseous mixtures "TeBr2 + Br2" and "I_2 + TeI_2": experimental (dots), calculated (line), and the difference $\Delta F(r)$ between experiment and theory.

However, this distance contributes poorly to the $sM(s)$ scattering intensities because of its large vibrational amplitude, long internuclear distance, single multiplicity, and low concentration (about 3% according to the MS data) of this molecular species in the vapor phase. Nevertheless, a refinement, at which the parameters of iodine were fixed at the optimized values while the contribution coefficient, internuclear distances, and vibration amplitudes of TeI_2 were refined, was undertaken. The R_f value decreased slightly from 2.9 to 2.5% and the least-squares procedure converged to a contribution $\alpha(TeI_2) = 0.049(7)$. This corresponds to a mol fraction with a $3\sigma_{LS}$ value of 3.3 ± 2.1 mol-% [as converted by Equation (1)]. The optimized molecular parameters of TeI_2 are r_g(Te–I) = 2.693(9), r_g(I···I) = 4.218(48), l(Te–I) = 0.059(6), and l(I···I) = 0.190(65) Å. The ∠I–Te–I angle is 103.1(22)°. Despite the low concentration of TeI_2 in the vapor, the refinement of its parameters was possible as a result of fixing the parameters for I_2 and as a result of the separated, although very weak, contribution of the I···I distance in the radial distribution function. Because of the low concentration, the standard deviations of all parameters are considerably larger than those for $TeBr_2$ (see Table 3).

Vapor Composition

$TeBr_4$(s)

Three possible net reactions may be considered for the evaporation process of tellurium tetrabromide under vacuum [Equation (2), Equation (3) and Equation (4)].

$$TeBr_4(s) \rightarrow TeBr_2(g) + Br_2(g) \quad (2)$$

$$TeBr_4(s) \rightarrow TeBr_4(g) \quad (3)$$

$$TeBr_4(s) = Te(s) + 2Br_2(g) \quad (4)$$

The composition of the vapor over solid $TeBr_4$, as determined by mass spectrometry (see Experimental Section), is 42.3:56.4:1.3 (L_1) and 41.1:57.7:1.2 mol-% (L_2) for $TeBr_2$/Br_2/$TeBr_4$. Taking into account the uncertainty of the intensities in the mass spectra, we estimated an inferior limit of uncertainties in the mol concentration, $x(TeBr_2)$ = 42.3 ± 2.3 mol-% (L_1) and 41.1 ± 0.9 mol-% (L_2). The value determined from the GED least-squares refinement was 38.3(6) mol-%. Both methods yielded similar results, although the values differ by slightly more than the combined error limits. This minor discrepancy might be caused by the fact that for conversion of α coefficients to mol concentrations, a simplified formula was applied that uses the "nuclear charge value approximation" (see, for example, Ref.[19]) for calculating the atomic scattering functions $I_{at}(s)$. Combination of the independent results from GED and MS leads to a concentration and estimated uncertainty of $x(TeBr_2) = 40(3)\%$.

Confirmation of the third gaseous product, $TeBr_4$, is given by the $TeBr_3^+$ ion in the mass spectra, which possesses very low intensity. This ion is supposed to be the most intense in the mass spectrum of $TeBr_4$, analogous to that found for TeF_4 and $TeCl_4$.[23] When calculating the concentration of the tetrabromide, the $TeBr_3^+$ intensity was multiplied by a factor of two to take into account the contributions from the fragmented ions parented by $TeBr_4$. This factor was estimated from the mass spectra of tetrafluoride and tetrachloride. We performed a series of the least-squares analyses of the GED data, in which a α_{TeBr4} contribution to the $sM(s)$ function [see Equation (1)] was considered in the refinement procedure. From the dependence of the discrepancy factor R_f vs. the fixed mol-% ($TeBr_4$) and from Hamilton's criterion approach,[24] the range for the tellurium tetrabromide concentration in the vapor under investigation was estimated to be about 1 mol-% or less, which does not contradict our MS data.

Basciani and Ferro[4] concluded from the torsion effusion method that the vaporization process at 423–485 K is described by $(x + y)TeBr_4(s) = xTeBr_4(g) + yTeBr_2(g) + yBr_2(g)$, where $x = 0.06$ and $y = 0.47$. This implies that 6% $TeBr_4$ is present in the vapor over solid $TeBr_4$, while $TeBr_2$ and Br_2 are the major molecular species with equal contributions. These results are similar to our MS and GED data at 471 K, although quantitatively slightly different.

TeI$_4$(s)

Both the GED and MS methods agree that at 373 K the vapor effusing from a cell filled with TeI_4(s) consists predominantly of I_2 with a minor contribution, about 3 mol-%, of TeI_2. This result is in agreement with the studies of Oppermann et al.[25] and D′Alessio et al.[5] that involve sublimation and decomposition of TeI_4. Therefore, two main processes take place on heating solid TeI_4 in vacuo [Equation (5) and Equation (6)].

$$TeI_4(s) \rightarrow 2I_2(g) + Te(s) \quad (5)$$

$$TeI_4(s) \rightarrow TeI_2(g) + I_2(g) \quad (6)$$

"Metallic" tellurium, as a possible decomposition product, can probably be excluded in the *gas* phase in both $TeBr_4$ and TeI_4 GED/MS experiments described in this work, since it is rather nonvolatile, as known from the literature. Tellurium possesses a saturated vapor pressure of 0.001 Torr at 595 K and 0.01 Torr at 647 K.[26] The temperature applied in the GED/MS experiment for $TeBr_4$ (471 K) and, even more so, that in the MS decomposition study of TeI_4 (373 K) are much lower. In case of TeI_4, an additional mass spectrometric study showed that only at temperatures above ca. 670 K did the ions Te^+ and Te_2^+ (the latter is most abundant) start to appear in the mass spectra. This is typical for chalcogens that are known to sublime as oligomers, Te_n, which first occurs as the dimer Te_2.

Geometric and Vibrational Parameters

The bond length r_g(Te–Br) = 2.480 ± 0.005 Å in $TeBr_2$ obtained in this study (Table 2) is consistent with the value r(Te–Br) = 2.49 ± 0.03 Å found by Grether[1] and close, but not consistent within the combined error limits, with the value of 2.51 ± 0.02 Å, reported by Rogers and Spurr.[2] With regard to the valence angle, it should be pointed out that in the first study the Br–Te–Br angle was estimated to be >150°,[1] and a value of 98 ± 3° was reported in the second study.[2] The latter agrees with our value of 99.0 ± 0.6°.

Although samples of TeX_2 (not TeX_4 as in our study) were used by Grether[1] and by Rogers and Spurr,[2] no direct evidence with regard to the vapor composition was available in those early GED works. It cannot be excluded that the vapor of $TeBr_2$ was "contaminated" with, for instance, molecular bromine or some other gaseous species.

The geometric and vibrational parameters of $TeBr_2$ determined in this work from analysis of the GED data may be used for testing the quality of various approximations applied in the quantum chemical (QC) calculations. In this work, we applied various combinations of methods and basis sets at levels higher than those published before. The results of QC calculations along with available experimental data are presented in Table 3. When the experimental and calculated bond lengths are compared, the systematic difference between the thermally averaged r_g and the equilibrium r_e distances has to be considered. Generally, r_e bond lengths are smaller than r_g values by a few thousandths of an Å. The difference between r_g and r_e distances can be estimated by the diatomic approximation of Kuchitsu,[27] $r_e = r_g - (3/2)a_3l^2$, which implies the neglecting of the perpendicular vibrations (according to the second approximation used in the SHRINK program), where a_3 is the asymmetry parameter and l the vibrational amplitude of the bond. Since no a_3 value for Te_2 is given,[27] we estimated it from the values for Se_2 (1.518 Å^{-1}), Br_2 (1.562 Å^{-1}), and I_2 (1.468 Å^{-1}).[27] Since Te is below Se in the periodic table and I below Br and a_3 for I_2 is slightly smaller than that for Br_2, we can estimate that a_3 for Te_2 should also be slightly smaller than that of Se_2, i.e. about 1.40 Å^{-1}. By using mean values of a_3 for Te_2 and X_2, the differences ($r_e - r_g$) and their uncertainties are estimated to be –0.008(2) Å for the Te–Cl and Te–Br bonds and –0.007(3) Å for the Te–I bond. For this estimate, experimental vibrational amplitudes were used for the Te–Br and Te–I bonds and an average of the calculated amplitudes for the Te–Cl bond [see Table 3, l(Te–Cl) = 0.057 Å]. With these corrections, experimental equilibrium distances of r_e(Te–Cl) = 2.323(4) Å, r_e(Te–Br) = 2.472(6) Å, and r_e(Te–I) = 2.686(10) Å are obtained. Comparison of these experimental r_e bond lengths with calculated values in Table 3 demonstrates that the MP2 method best reproduces these values, the CCSD and CCSD(T) methods slightly overestimate the experimental values, and the B3LYP method strongly overestimates them.

The valence angles predicted by the B3LYP method are by 1–2° larger than the experimental values, with the exception of that in TeI_2, which possesses a large uncertainty. All other methods applied reproduce the GED values more closely. The *covalent radii* of the elements constituting the molecules of interest possess values of 1.35 for Te and 0.64, 0.99, 1.14, and 1.33 Å for the halogens F, Cl, Br, and I, respectively.[28] The sum of the covalent radii gives an estimation of the Te–X bond lengths, r(Te–F) = 1.99 Å, r(Te–Cl) = 2.34 Å, r(Te–Br) = 2.49 Å, and r(Te–I) = 2.68 Å. These estimates are very close to the experimental and QC values for chloride, bromide, and iodide, which confirms a practically pure covalent character of the chemical bonds in these tellurium dihalides. The exception is fluoride, for which this sum overestimates the bond length by about 0.1 Å relative to the quantum chemical values. Qualitatively, the large difference between the sum of the covalent radii and QC predictions can be rationalized by a high ionic (or polar) contribution, Te^+–F^-. A strong increase in the positive atomic charge at the Te atom from TeI_2 to TeF_2 is shown in Figure 2. A similar situation is also observed for SeF_2, where the sum of the covalent radii is larger than the predicted value by 0.07 Å. These discrepancies make GED/MS experiments for the chalcogen difluorides highly desirable.

The results of this study and of our recent work on selenium dihalides[29] strongly supplement the experimental and theoretical data on the structural parameters of chalcogen dihalides compiled previously.[28] In this context it should be pointed out that the stepwise decrease in the valence angle X–E–X in chalcogen dihalides in the series

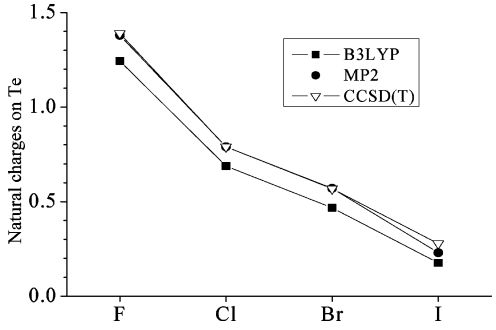

Figure 2. Natural charges on the Te atom in TeX_2 molcules (X = F, Cl, Br, I) as calculated in the NBO analysis by different theoretical approaches.

S→Se→Te is now more evident and is confirmed. The step is about –2°, independent of the halogens. A very similar trend has been observed for other ligands, such as CH_3 and CF_3.

A comparison between the experimental and calculated vibrational parameters can be performed only in the case of $TeCl_2$, the only chalcogen dihalide for which gas-phase vibrational frequencies from Raman spectroscopy have been reported[6] (see Table 3). This comparison demonstrates that MP2 overestimates the symmetric stretching frequency by about 8%, whereas all other approximations reproduce the experimental value closely. The frequency for the symmetric deformation is less sensitive towards the computational method. It should be pointed out that the B3LYP method in combination with ECP-46 on Te perfectly reproduces the ν_1 and ν_2 values of the Raman spectra. A set of frequencies[30] based on MP2/6-31G* calculations (381, 132, and 367 cm^{-1}) and scaled frequencies (378, 121, and 364 cm^{-1}) using scaling factors from $TeCl_4$ reproduces the experimental values very well.

In addition to the comparison of experimental and calculated frequencies, we can compare vibrational amplitudes derived by GED with those calculated from quantum chemical force fields by using the SHRINK program of Sipachev.[21] This comparison allows an estimate of the quality of the force fields calculated by the different QC methods. In Table 3, vibrational amplitudes *l*(Te–X) and *l*(X···X) obtained by experiment and QC calculations are listed for X = Cl and Br. In the case of Br, good agreement with theoretical predictions exists for both amplitudes. For $TeCl_2$, the (Cl···Cl) amplitude from GED is reproduced well by theory, but all calculated *l*(Te–Cl) values of 0.054 to 0.059 Å are considerably smaller than the GED result [0.070(2) Å].[3] This experimental value seems to be too large for some reason; this is also the case for $TeBr_2$ and TeI_2, and therefore a mean calculated amplitude was used above to estimate the ($r_g - r_e$) correction.

Natural Bond Orbital (NBO) Analysis

We performed an analysis of the electron density distribution in terms of natural bond orbitals (NBO)[17] for the molecules TeX_2 (X = F, Cl, Br, I). According to the NBO analysis, the electron lone pairs of tellurium in TeX_2 are nonequivalent and possess different energies. The first pair, $LP_1(Te) = sp_z^{0.12}$ (symmetry a_1), represents the 5s atomic orbital (AO), partially polarized along the symmetry axis *z*. The second pair, $LP_2(Te) = p_x$ (symmetry b_1), represents the AO in which the electron density maxima are symmetrically localized above and below the *yz* molecular plane and has no influence on the orbitals in the *yz* plane. Thus, the mutual orientation of the three electron density domains in the *yz* plane, the $LP_1(Te)$ and the two hybrid *h*(Te) AOs taking part in the formation of the localized σ(Te–X) molecular orbitals (MOs), determines the value of the valence angle, rather than the orientations of the four electron density domains on Te discussed in the VSEPR model.[28] This suggestion was recently discussed by Haaland.[31]

The valence angle depends primarily on the composition of the *h*(Te) hybrid AOs and $LP_1(Te)$. These compositions are almost equal in all TeX_2 (X = F, Cl, Br, I) molecules (Table 4). The area which $LP_1(Te)$ occupies in the *yz* plane is significantly larger than that of the *h*(Te) orbitals. Therefore, the valence angle X–Te–X is close to 100° and is significantly smaller than the ideal angle of 120° between three equivalent domains in a plane. The slight increase in the X–Te–X valence angle in the series TeF_2–TeI_2 (see Table 3) cannot be attributed to an increase in repulsion between the halogen atoms. The *r*(X···X) distances in all dihalides exceed the corresponding sum of "one-angle"-nonbonded radii (r_{1-3}) equal to 1.08, 1.44, 1.59, and 1.86 Å for F, Cl, Br, and I, respectively.[28] Therefore, we suggest that this trend in the valence angles is due to different electronegativities (EN) of the ligands. A decrease in the EN of the substituent is accompanied by a decrease in the coefficient at the *h*(X) hybrid orbital and by a simultaneous increase in the coefficient of the *h*(Te) hybrid in the σ(Te–X) bonding MO. As a consequence, the volume occupied by two *h*(Te) hybrid orbitals at the valence shell of the central atom increases, which leads to an increase in the X–Te–X angle as the EN of the ligand decreases. This is in agreement with the VSEPR model.[28] According to this model, a ligand with a higher EN attracts the electron density of the shared bonding pair, which then decreases the volume of the electron density in the valence shell of the central atom, and, thus, decreases the repulsion between the shared pairs. This finally leads to a decrease in the valence angle. This statement of the VSEPR model is clearly demonstrated by the coeffi-

Table 4. Localized two-centered MOs σ(Te–X) and the composition of the hybrid AOs for Te and X (X = F, Cl, Br, I) according to CCSD(T)/ECP-46 calculations.

	Localized two-centered MOs	Hybrid AO composition
TeF_2	σ(Te–F) = 0.37*h*(Te)+ 0.93*h*(F)	*h*(Te) = $s^{0.06}p^1$
	σ*(Te–F) = 0.93*h*(Te)–0.37*h*(F)	*h*(F) = $s^{0.24}p^1$
$TeCl_2$	σ(Te–Cl) = 0.54 *h*(Te)+0.84*h*(Cl)	*h*(Te) = $s^{0.06}p^1$
	σ*(Te–Cl) = 0.84*h*(Te)–0.54*h*(Cl)	*h*(Cl) = $s^{0.13}p^1$
$TeBr_2$	σ(Te–Br) = 0.59*h*(Te)+0.81*h*(Br)	*h*(Te) = $s^{0.06}p^1$
	σ*(Te–Br) = 0.81*h*(Te)–0.59*h*(Br)	*h*(Br) = $s^{0.09}p^1$
TeI_2	σ(Te–I) = 0.65*h*(Te)+0.76*h*(I)	*h*(Te) = $s^{0.06}p^1$
	σ*(Te–I) = 0.76*h*(Te) – 0.65*h*(I)	*h*(I) = $s^{0.07}p^1$

cients of the *h*(Te) and *h*(X) AOs in the linear combination of localized σ(Te–X) MOs (see Table 4). Decrease in the EN of the substituent is accompanied by a decrease in the coefficient at the *h*(X) hybrid orbital and by a simultaneous increase in the coefficient of the *h*(Te) hybrid in the σ(Te–X) bonding MO. As a consequence, the volume occupied by two *h*(Te) hybrid orbitals at the valence shell of the central atom increases, which leads to an increase in the X–Te–X angle as the EN of the ligand decreases.

Experimental Section

GED/MS

$TeBr_4$: The combined GED/MS experiment was carried out by using the technique described earlier.[7] The vapor effused from a graphite cell; the orifice had internal dimensions of 0.6 mm × 1.2 mm (diameter × length). The ratio of the evaporation/effusion areas exceeded 500. The temperature as measured by a W–Re (5/20) thermocouple was 471(5) K. All operations with the sample $TeBr_4$ (a yellow–orange fine-grained powder, Aldrich, 99.999%, anhydrous, m.p. 653 K) were carried out in a glove box dried by P_2O_5.

The scattered electrons were collected on Kodak Electron Image films of 9 × 12 cm. Six films from each of the two camera distances, L_1 = 598 and L_2 = 338 mm, were taken for analysis. The optical densities were measured by a computer-controlled MD-100 (Carl Zeiss, Jena) microdensitometer.[8] The molecular scattering function was evaluated as $sM(s) = [I(s)/G(s) - 1]\cdot s$, where $I(s)$ is the total electron scattering intensity and $G(s)$ the experimental background. For the vapor over solid $TeBr_4$, the experimental and theoretical radial distribution curves $F(r)$ along with their difference curve $\Delta F(r)$ are shown in Figure 1.

After crossing the electron beam, the molecular beam effusing from the cell enters directly into the ionization chamber of a monopole mass spectrometer attached to the GED unit. This provided a real-time monitoring of the vapor composition by recording of the mass spectra simultaneously with the taking of the diffraction patterns. The mass spectra (Table 1) demonstrate that the sample of $TeBr_4$ evaporates incongruently, decomposing to tellurium dibromide, $TeBr_2$, and molecular bromine, Br_2, along with a small amount of tellurium tetrabromide, $TeBr_4$.

TeI_4: A sample of TeI_4 was purchased from Aldrich, no grade indicated, black crystals of 0.5–2.5 mm size, with metallic shining. The crystals appeared to be insoluble in water and slowly soluble in ethanol. All operations with the sample were carried out in a glove box dried by P_2O_5. The same graphite effusion cell, as used for $TeBr_4$, was kept at 373 K during the recording of the diffraction patterns. Conditions of the combined apparatus operations were similar to those for $TeBr_4$.

Mass spectra (U_i = 50 V) of the vapor over solid TeI_4 consisted of the following peaks: 48 (I^+), 100 (I_2^+), 4 (TeI^+), 2 (TeI_2^+); the relative intensities take the natural isotopic abundances into account. This demonstrates that almost complete decomposition into I_2 takes place with a minor amount of TeI_2 at a "trace" level. For the vapor over solid TeI_4, the experimental and theoretical radial distribution curves $F(r)$ along with their difference $\Delta F(r)$ are shown in Figure 1.

Analyses of the mass spectra for the both compounds showed no peaks other than those mentioned in Table 1 ($TeBr_4$) and in the text above (TeI_4), which guarantees, in our case, a purity of 99%, at least.

Quantum Chemical Calculations

All quantum chemical calculations were performed with the program set GAUSSIAN 03.[9] The density functional theory method (DFT-B3LYP), the Møller-Plesset perturbation theory of the second order (MP2), and the coupled-cluster method with all single and double excitations (CCSD) and a perturbative estimate of the triple excitations [CCSD(T)] were applied. The MP2, CCSD, and CCSD(T) calculations were carried out by using the chemical "frozen" core approach.

For tellurium the large, 46 electron ($1s^22s^22p^63s^23p^63d^{10}4s^24p^64d^{10}$),[10] and small, 28 electron ($1s^22s^22p^63s^23p^63d^{10}$),[11] core shells were described by the relativistic effective core potentials, abbreviated onward as ECP–46 and ECP–28, respectively. The (15s,11p,3d,1f)/[3s,3p,2d,1f][12] and (12s11p9d1f)/[5s4p3d1f][11] basis sets (cc-pVTZ) were used for the outer shell description supplemented by diffuse s, p, d, and f functions (aug-cc-pVTZ), in combination with the ECP–46 and ECP–28 effective potentials, respectively.

The (11s6p3d2f)/[5s4p3d2f][13] and (16s10p3d2f)/[6s5p3d2f][14] full-electron correlation consistent polarized valence basis sets augmented by diffuse functions (aug-cc-pVTZ) were applied for the F and Cl atoms, respectively. For bromine and iodine, the core shells [($1s^22s^22p^63s^23p^63d^{10}$) for Br and ($1s^22s^22p^63s^23p^63d^{10}4s^24p^64d^{10}$) for I] were described by relativistic effective core potentials,[10] and (14s10p2d1f)/[3s3p2d1f] basis sets supplemented by diffuse s, p, d, and f functions[12] were used for the description of the valence shells.

The parameters of pseudopotentials and basis sets were taken from the database,[15] with the exception of the ECP–28 pseudopotentials on the Te atom and the corresponding basis set, which were taken from the database.[16]

The most extensive calculations were performed for $TeBr_2$ in order to compare results of various theoretical approximations with those from our GED/MS study. Since $TeBr_4$ has been detected in the vapor over solid tellurium tetrabromide, although in quite small amounts, quantum chemical calculations were performed for this molecule, including those at the B3LYP and MP2 levels with ECP-46 combination of core shell and basis sets. In addition, an electron density distribution analysis in terms of natural bond orbitals (NBO)[17] was performed by using the option implemented into the Gaussian package.

Acknowledgments

We thank the Deutsche Forschungsgemeinschaft, DFG (413 RUS 113/69/0–6) and Russian Foundation for Basic Research, RFBR (grant 07–03–91561-HHNO_a) for financial support of the Russian–German Cooperation.

[1] W. Grether, *Ann. Phys.* **1936**, *418*, 1–16.
[2] M. T. Rogers, R. A. Spurr, *J. Am. Chem. Soc.* **1947**, *69*, 2102–2103.
[3] L. Fernholt, A. Haaland, H. V. Volden, R. Kniep, *J. Mol. Struct.* **1985**, *128*, 29–31.
[4] S. Basciani, L. D'Alessio, D. Ferro, *J. Alloys Compd.* **1995**, *230*, 63–6.
[5] L. D'Alessio, D. Ferro, V. Piacente, *J. Alloys Compd.* **1994**, *209*, 207–212.
[6] I. R. Beattie, R. O. Perry, *J. Chem. Soc. A* **1970**, *14*, 2429–2432.

[7] G. V. Girichev, A. N. Utkin, Yu. F. Revichev, *Prib. Tekh. Eksp.* **1984**, *2*, 187–190 (Russian); G. V. Girichev, S. A. Shlykov, Yu. F. Revichev, *Prib. Tekh. Eksp.* **1986**, *4*, 167–169 (Russian).
[8] E. G. Girichev, A. V. Zakharov, G. V. Girichev, M. I. Bazanov, *Izv. Vysh. Uchebn. Zaved., Technol. Text. Prom.* **2000**, *2*, 142–146 (Russian).
[9] M. J. Frisch, G. W. Trucks, H. B. Schlegel, G. E. Scuseria, M. A. Robb, J. R. Cheeseman, J. A. Montgomery Jr, T. Vreven, K. N. Kudin, J. C. Burant, J. M. Millam, S. S. Iyengar, J. Tomasi, V. Barone, B. Mennucci, M. Cossi, G. Scalmani, N. Rega, G. A. Petersson, H. Nakatsuji, M. Hada, M. Ehara, K. Toyota, R. Fukuda, J. Hasegawa, M. Ishida, T. Nakajima, Y. Honda, O. Kitao, H. Nakai, M. Klene, X. Li, J. E. Knox, H. P. Hratchian, J. B. Cross, C. Adamo, J. Jaramillo, R. Gomperts, R. E. Stratmann, O. Yazyev, A. J. Austin, R. Cammi, C. Pomelli, J. W. Ochterski, P. Y. Ayala, K. Morokuma, G. A. Voth, P. Salvador, J. J. Dannenberg, V. G. Zakrzewski, S. Dapprich, A. D. Daniels, M. C. Strain, O. Farkas, D. K. Malick, A. D. Rabuck, K. Raghavachari, J. B. Foresman, J. V. Ortiz, Q. Cui, A. G. Baboul, S. Clifford, J. Cioslowski, B. B. Stefanov, G. Liu, A. Liashenko, P. Piskorz, I. Komaromi, R. L. Martin, D. J. Fox, T. Keith, M. A. Al-Laham, C. Y. Peng, A. Nanayakkara, M. Challacombe, P. M. W. Gill, B. Johnson, W. Chen, M. W. Wong, C. Gonzalez, J. A. Pople, *Gaussian 03*, Revision B.03, Gaussian, Inc., Pittsburgh PA, **2003**.
[10] A. Bergner, M. Dolg, W. Kuechle, H. Stoll, H. Preuss, *Mol. Phys.* **1993**, *80*, 1431–1441.
[11] K. A. Peterson, D. Figgen, E. Goll, H. Stoll, M. Dolg, *J. Chem. Phys.* **2003**, *119*, 11113–11123.
[12] J. M. L. Martin, A. Sundermann, *J. Chem. Phys.* **2001**, *114*, 3408–3420.
[13] T. H. Dunning Jr, *J. Chem. Phys.* **1989**, *90*, 1007–1023; R. A. Kendall, T. H. Dunning Jr, R. J. Harrison, *J. Chem. Phys.* **1992**, *96*, 6796–6809.
[14] D. E. Woon, T. H. Dunning Jr, *J. Chem. Phys.* **1993**, *98*, 1358–1371.
[15] The Extensible Computational Chemistry Environment Basis Set Database, Version 6/19/03, developed and distributed by the Molecular Science Computing Facility, Environmental and Molecular Sciences Laboratory, P. O. Box 999, Richland, Washington 99352, USA, and funded by the U. S. Department of Energy. http://www.emsl.pnl.gov/forms/basisform.html.
[16] Pseudopotentials of the Stuttgart/Cologne group, http://www.theochem.uni-stuttgart.de.
[17] J. E. Carpenter, F. Weinhold, *THEOCHEM* **1988**, *169*, 41–62; A. E. Reed, L. A. Curtiss, F. Weinhold, *Chem. Rev.* **1988**, *88*, 899–926.
[18] B. Andersen, H. M. Seip, T. G. Strand, R. Stølevik, *Acta Chem. Scand.* **1969**, *23*, 3224–3234.
[19] G. V. Girichev, *Zh. Fiz. Khim.* **1989**, *LXIII*, 2273–2276 (Russian).
[20] K. S. Krasnov (Ed.), *Molecular Constants of Inorganic Compounds – Handbook*, Khimia, Leningrad, **1979**, p. 448 (Russian).
[21] V. A. Sipachev, *J. Mol. Struct.* **2001**, *567*, 67–72; V. A. Sipachev, *J. Mol. Struct.* **1985**, *121*,143–151.
[22] T. Ukaji, K. Kuchitsu, *Bull. Chem. Soc. Jpn.* **1966**, *39*, 2153–2156.
[23] N. I. Giricheva, S. A. Shlykov, A. V. Titov, D. Lentz, G. V. Girichev, *XX Austin Symp. on Mol. Struct., March 1–4*, Austin, **2008**, 78.
[24] W. C. Hamilton, *Acta Crystallogr.* **1965**, *18*, 502–510.
[25] H. Oppermann, G. Stoever, E. Wolf, *Z. Anorg. Allg. Chem.* **1976**, *419*, 200–212.
[26] A. I. Efimov (Ed.), *Properties of Inorganic Compounds–Handbook*, Khimia, Leningrad, **1983**, p. 392 (Russian).
[27] K. Kuchitsu, M. Nakata, S. Yamamoto in *Stereochemical Applications of Gas-Phase Electron Diffraction, Part A* (Eds.: I. Hargittai, M. Hargittai), VCH, Weinheim, **1988**, 227.
[28] R. J. Gillespie, I. Hargittai, *The* VS*EPR Model of Molecular Geometry*, Allyn and Bacon, **1991**.
[29] S. A. Shlykov, A. V. Titov, H. Oberhammer, N. I. Giricheva, G. V. Girichev, "The Molecular Structure of Selenium Dibromide as Deteremined by Combined Gas-Phase Electron Diffraction – Mass Spectrometric Experiment and Quantum Chemical Calculations", *Phys. Chem. Chem. Phys.* **2008**, DOI:10.1039/B808071B.
[30] A. Kovacs, R. J. M. Konings, *J. Mol. Struct.* **1997**, *410–411*, 407–410.
[31] A.Haaland, *Molecules and Models. The Molecular Structures of Main Group Element Compounds*, Oxford University Press, Oxford, **2008**, p. 330.

Received: July 15, 2008
Published Online: October 20, 2008

